Measurement-Based Robust Stability Assessment of Interconnections Using Impedance Models

1st Dmitry Rimorov
Dept. of Power Electronics in Grids
Hydro-Québec Research Institute
Varennes, Canada
rimorov.dmitry@hydroquebec.com

2nd James R. Forbes
Dept. of Mechanical Engineering
McGill University
Montréal, Canada
james.richard.forbes@mcgill.ca

3rd Richard Gagnon
Dept. of Power Electronics in Grids
Hydro-Québec Research Institute
Varennes, Canada
gagnon.richard2@hydroquebec.com

***Abstract*—Impedance model-based stability assessment is a popular approach for interconnection studies and is often complementary to full-scale simulation studies. It can be of great utility when only frequency response measurements are available. Given that the stability assessment must be done for various operating points and network conditions, it is of great importance to develop tools that give the most information about relevant stability margins and robustness metrics, especially when there are few measurements available. The paper applies the structured singular value analysis methodology for robust stability assessment of converter-based generation interconnection to electric grids. It is shown that in some important cases the associated uncertainty models can be refined to provide tight bounds on robust stability metrics. The proposed approach is demonstrated for a case of wind-park interconnection to a series-compensated grid to analyze subsynchronous control interactions. The results confirm the practical utility of the described methodology.**

***Index Terms*—Grid-connected inverters, impedance models, power systems stability, robust stability, structured uncertainty**

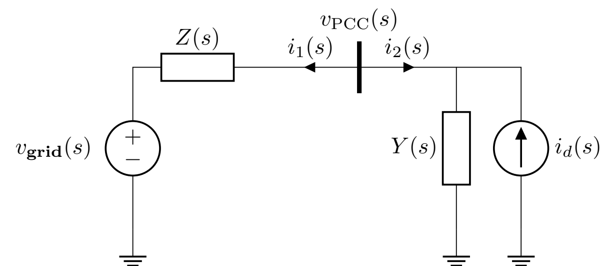

Fig. 1: Network equivalents' representation of interconnection.

I. Introduction

Impedance-based stability analysis techniques comprise a set of methods that rely on measuring equivalent impedance/admittance characteristics of the interconnected subsystems. Such methods can be useful when analytical models are either not available or are too difficult to derive, but direct measurements are relatively easy to obtain. Examples include manufacturer-specific black-box models of controllers [1] or full-scale control systems' replicas [2], physical devices that can be connected to a programmable source [3], Electromagnetic Transient (EMT) models of a grid with a particular Point of Common Coupling (PCC) [4], and others.

The basis of such methods lies in identifying the Thevenin and Norton equivalents of the interconnected subsystems at the PCC, as shown in Fig. 1. For the case of three-phase systems such models can be established in various domains, including dq, $\alpha\beta$ and phasor representation [5]. Whatever the modelling approach adopted, stability of the interconnection is then checked by validating the internal stability of the associated feedback loop [6]. In the context of frequency response data the generalized Nyquist stability criterion is typically used [4], [7], [8].

It can be argued that in its current form the impedance scanning techniques are of limited utility when a large set of operating conditions needs to be assessed, such as in interconnection studies. The MIMO Nyquist stability criterion, even when applied correctly, does not provide any reliable stability margins [9]. Therefore, each operating point must be validated individually. This process can be time consuming, offering little advantage over direct simulations.

Thus, there is a need to develop efficient approaches for robust stability analysis when there are few measurements available. One tool is small gain theorem, which provides a sufficient condition for robust stability [10], albeit in a conservative manner. If model uncertainty has a particular structure, more refined analysis using structured singular value (SSV) is possible [11]. Alternative methods involve passivity-based analysis by checking positive-realness of the impedance in the frequency range of interest [12]. Combined hybrid passivity and small gain stability criteria checks are a nice extension of such approaches [13], [14], but again have a tendency to produce a conservative estimation.

The contribution of this paper lies in applying the SSV, or μ-analysis for robust stability assessment of the interconnections using impedance measurements. Practical cases that involve interconnection studies of IBRs with electrical grids are the primary focus. The use of different modelling domains is emphasized to potentially reduce the conservatism of the analysis. A general procedure of robust stability assessment from limited number of measurements is formulated. A more refined analysis is then proposed for particular scenarios where certain information about the nature of the perturbation is available. The method is demonstrated on a problem of subsynchronous control interactions (SSCI) of a wind park connected to the

979-8-3315-8138-1

grid through a series-compensated transmission line.

The paper is organized as follows. Section II introduces the notation used in the paper. Section III discusses the perturbed model approach for uncertainty and the associated SSV analysis. Section IV summarizes two modelling approaches for three-phase circuit representation in either stationary or rotating reference frames. Section V outlines the procedure for robust stability. Section VI presents the results. Section VII concludes the paper.

II. Notation

This section establishes the notation used in the paper. MIMO impedance and admittance transfer functions are identified using symbols Z and Y, respectively, while G is used for a general system. The term "impedance" is used to refer to either impedance or admittance, depending on the context. Unknown stable and norm bounded transfer functions used to capture model uncertainties are denoted with the symbol Δ, and δ is an unknown norm bounded scalar that represents parametric uncertainty. The set of stable rational transfer matrices is denoted $\mathcal{RH}_\infty$. Upper and lower Linear Fractional Transformations (LFTs) for a transfer matrix partitioned as

$$P = \begin{bmatrix} P_{11} & P_{12} \\ P_{21} & P_{22} \end{bmatrix}$$

are defined as [15]

$$\mathcal{F}_u\left(P, \Delta_u\right) = P_{22} + P_{21}\Delta_u \left(I - P_{11}\Delta_u\right)^{-1} P_{12},$$
$$\mathcal{F}_l\left(P, \Delta_l\right) = P_{11} + P_{12}\Delta_l \left(I - P_{22}\Delta_l\right)^{-1} P_{21}.$$

These are useful to represent closed-loop maps in systems with feedback interconnections.

The frequency of the rotating reference frame is identified with ω_0. Bold symbols are reserved for complex vectors and complex transfer functions. A frequency shift operator for a complex vector or a complex transfer function is defined as $\mathrm{S}_\omega : \mathbf{u}(s) \rightarrow \mathbf{u}(s + j\omega)$. The symbol * is used for a complex-conjugate of a complex vector or a complex transfer function.

From now on, the argument "s" will be omitted and the Laplace domain is assumed, unless explicitly stated.

III. Impedance uncertainty modelling for robust stability analysis

Robust stability analysis requires introducing variations of the plant model that represent modelling errors or deviations from an operating point. A perturbed model approach is a standard tool for such representation. For instance, the perturbed model of the grid impedance is a set of upper LFT

$$Z_\mathrm{p} := \{\mathcal{F}_u\left(Z_0, \Delta_\mathrm{Z}\right) :\ \Delta_\mathrm{Z} \in \mathcal{RH}_\infty,\ \|\Delta_\mathrm{Z}\|_\infty\ < 1\}. \tag{1}$$

The form of Z_0 depends on the chosen uncertainty model. A particular grid model is recovered by properly choosing Δ_Z. If $\Delta_\mathrm{Z} = 0$ a nominal plant is recovered. Such representation can ether be derived analytically for known transfer functions, or established from frequency response measurements.

The same modelling approach can be adopted to represent the perturbed model of Y as a lower LFT. The overall representation of the interconnection for such modelling approach is shown in Fig. 2. The interconnection of Fig. 2 is a cascade

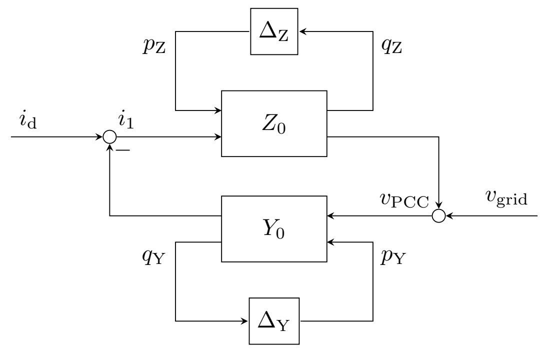

Fig. 2: Perturbed model representation of interconnection.

of LFTs, which is itself an LFT $F = \mathcal{F}_u\left(N, \Delta\right)$, where $\Delta = \mathrm{diag}\{\Delta_\mathrm{Z}, \Delta_\mathrm{Y}\}$. The μ-analysis theory states that the closed-loop system will be stable for any pair of perturbations $\Delta_\mathrm{Z}, \Delta_\mathrm{Y}$ if nominal interconnection is stable and the structured singular value (SSV) $\mu_\Delta(M) < 1$, where $q = Mp$ and the SSV is defined as

$$\mu_\Delta(M) := \frac{1}{\min\{\bar{\sigma}(\Delta) : \Delta \in \boldsymbol{\Delta}, \det(I - M\Delta) = 0\}}.$$

The set $\boldsymbol{\Delta}$ is the set of all perturbations of a given structure. Simply put, the SSV analysis relieves the conservatism of the small gain theorem by exploiting the perturbation structure [11]. In practice, lower and upper bounds of the SSV are calculated

$$\underline{\mu}_\Delta(M) \leq \mu_\Delta(M) \leq \bar{\mu}_\Delta(M).$$

For the model of Fig. 2, Δ is block-diagonal. However, to improve the robust stability analysis, further structure in Δ_Z and Δ_Y should be sought out and leveraged. The structure can be the result of the choice of the domain that is used to represent the impedance of the systems. The next section elaborates on two different ways to model the impedance considered in this paper.

IV. Impedance modelling in different domains

A 3-phase LTI circuit in dq-domain can be described in matrix form as

$$\begin{bmatrix} y_d \\ y_q \end{bmatrix} = \begin{bmatrix} G_{dd} & -G_{dq} \\ G_{qd} & G_{qq} \end{bmatrix} \begin{bmatrix} u_d \\ u_q \end{bmatrix}. \tag{2}$$

Introducing the notation of the complex transfer functions (CTFs) [16]

$$\mathbf{G}_+^{dq} = \frac{G_{dd} + G_{qq}}{2} + j\frac{G_{dq} + G_{qd}}{2}$$
$$\mathbf{G}_-^{dq} = \frac{G_{dd} - G_{qq}}{2} + j\frac{G_{qd} - G_{dq}}{2},$$

(2) can be compactly represented as

$$\mathbf{y}^{dq} = \mathbf{G}_+^{dq}\mathbf{u}^{dq} + \mathbf{G}_-^{dq}\left(\mathbf{u}^{dq}\right)^*. \tag{3}$$

979-8-3315-8138-1

Translating to the stationary $\alpha\beta$-frame gives

$$\mathrm{S}_{\omega_0}\left(\mathbf{y}^{\alpha\beta}\right) = \mathbf{G}_{+}^{dq}\left(\mathrm{S}_{\omega_0}\left(\mathbf{u}^{\alpha\beta}\right)\right) + \mathbf{G}_{-}^{dq}\left(\mathrm{S}_{\omega_0}\left(\mathbf{u}^{\alpha\beta}\right)\right)^*,$$

which after applying $\mathrm{S}_{-\omega_0}$ is equivalent to

$$\mathbf{y}^{\alpha\beta} = \mathrm{S}_{-\omega_0}\left(\mathbf{G}_{+}^{dq}\right)\mathbf{u}^{\alpha\beta} + \mathrm{S}_{-\omega_0}\left(\mathbf{G}_{-}^{dq}\right)\left(\mathrm{S}_{-2\omega_0}\left(\mathbf{u}^{\alpha\beta}\right)\right)^*. \tag{4}$$

Thus, the asymmetry in dq domain creates cross-coupling between frequencies ω and $2\omega_0 - \omega$ in the stationary reference frame.

A pair of frequencies $(\omega, -\omega)$ and $(\omega, 2\omega_0 - \omega)$ for (3) and (4) respectively is enough to describe the systems' response. This allows for an alternative description of the system. Specifically, taking complex-conjugate of (3) allows the following representation using a 2×2 complex transfer matrix

$$\begin{bmatrix} \mathbf{y}^{dq} \\ \left(\mathbf{y}^{dq}\right)^* \end{bmatrix} = \underbrace{\begin{bmatrix} \mathbf{G}_{+}^{dq} & \mathbf{G}_{-}^{dq} \\ \left(\mathbf{G}_{-}^{dq}\right)^* & \left(\mathbf{G}_{+}^{dq}\right)^* \end{bmatrix}}_{\bar{\mathbf{G}}^{dq}} \begin{bmatrix} \mathbf{u}^{dq} \\ \left(\mathbf{u}^{dq}\right)^* \end{bmatrix}. \tag{5}$$

This is a modified sequence representation [7]. Similarly, applying $\mathrm{S}_{-2\omega_0}$ to (4) and taking its complex-conjugate results in the following form in $\alpha\beta$-domain

$$\begin{bmatrix} \mathbf{y}^{\alpha\beta} \\ \left(\mathrm{S}_{-2\omega_0}\left(\mathbf{y}^{\alpha\beta}\right)\right)^* \end{bmatrix} = \underbrace{\mathrm{S}_{-\omega_0}\left(\bar{\mathbf{G}}^{dq}\right)}_{\bar{\mathbf{G}}^{\alpha\beta}} \begin{bmatrix} \mathbf{u}^{\alpha\beta} \\ \left(\mathrm{S}_{-2\omega_0}\left(\mathbf{u}^{\alpha\beta}\right)\right)^* \end{bmatrix}, \tag{6}$$

which is the expression of the unified impedance modelling framework proposed in [17].

Equations (2) and (6) are equivalent representations of a three-phase circuit in dq and $\alpha\beta$ domains, respectively, and would produce identical stability assessment results when using the generalized Nyquist stability criterion [17]. Indeed, (6) is obtained from (2) by a linear transformation and a frequency shift. However, for the purpose of SSV analysis presented in the next section, the choice of the modelling domain can have an impact due to the structure of the resulting impedance matrix. For example, $\bar{\mathbf{G}}^{\alpha\beta}$ is diagonal for balanced grids. In general, having a more structured model can reduce the conservatism of the general procedure formulated in the following section.

V. Robust stability assessment with uncertainty structure

A. The general procedure

When no information about the model uncertainty is given besides a few frequency response measurements, the most general procedure of robust stability assessment aims at constructing a smallest possible set that contains all the measured responses. It proceeds as follows.

1) Obtain N_{G} frequency response measurements of the subsystems' impedance models, resulting in a set of MIMO frequency responses $H_k = \{G_1(j\omega_k), \ldots, G_{N_{\mathrm{G}}}(j\omega_k)\}$ for each frequency ω_k. SISO frequency response of each input-output pair is in the set $H_k^{i,j}$. At this stage, some idea about system characteristics can help determining the best modelling approach.
2) Construct the perturbed models for each subsystem by choosing a nominal plant and identifying a proper uncertainty model. Concerning nominal plant choice, a sensible approach is to find an average model as follows
$$G_{\mathrm{nom}}(j\omega_k) = \frac{\sum_{\ell=1}^{N_{\mathrm{G}}} G_\ell(j\omega_k)}{N_{\mathrm{G}}}.$$
Then the worst case deviation is a point-wise maximum for each input-output pair at a given frequency
$$G_{\mathrm{wc}}^{i,j}(j\omega_k) = \underset{G^{i,j} \in H_k^{i,j}}{\operatorname{argmax}} |G^{i,j}(j\omega_k) - G_{\mathrm{nom}}^{i,j}(j\omega_k)|.$$
Having obtained both nominal and worst case deviation models, LFT description needs to be established by fitting one of the common form uncertainty models shown in Fig. 3. This is done by evaluating the weight blocks on a frequency-by-frequency basis from previously calculated $G_{\mathrm{nom}}^{i,j}$ and $G_{\mathrm{wc}}^{i,j}$ using the relations indicated in Fig. 3. The weight with the smallest $\mathcal{H}_\infty$ norm determines the uncertainty model structure. To complete the SISO perturbed model, a $\Delta^{i,j}$ block satisfying conditions in (1) is added in series with the calculated weight. Subsequent LFT representation for the entire MIMO system is done by "pulling out" the $\Delta^{i,j}$ blocks and arranging them in a diagonal structure [18, Chapter 8]. Each $\Delta^{i,j}$ is assumed to be different.
3) Evaluate nominal stability of the interconnection with the nominal models from the previous step using the generalized Nyquist stability criterion.
4) Calculate the SSV upper and lower bounds for a given uncertainty structure to evaluate robust stability for the constructed perturbed model. If the upper SSV bound is below 1, the robust stability is guaranteed.

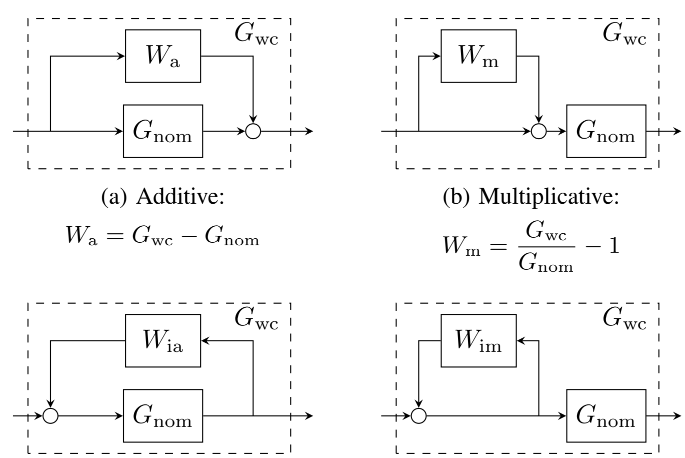

(a) Additive: $W_{\mathrm{a}} = G_{\mathrm{wc}} - G_{\mathrm{nom}}$

(b) Multiplicative: $W_{\mathrm{m}} = \dfrac{G_{\mathrm{wc}}}{G_{\mathrm{nom}}} - 1$

(c) Inverse Additive: $W_{\mathrm{ia}} = \dfrac{1}{G_{\mathrm{nom}}} - \dfrac{1}{G_{\mathrm{wc}}}$

(d) Inverse Multiplicative: $W_{\mathrm{im}} = 1 - \dfrac{G_{\mathrm{nom}}}{G_{\mathrm{wc}}}$

Fig. 3: SISO uncertainty models and weights calculations. Calculations are performed on a frequency-by-frequency basis

979-8-3315-8138-1

The procedure outlined in this section tends to produce conservative estimates of minimum destabilizing perturbations. By design, the resulting perturbed model contains all the measured responses. However, it also contains the instances of the impedance-based models that are not part of H_k. Some of these models may not be physically realizable. Next subsection proposes how to refine the robust stability assessment for some special cases important in practice.

B. Particular cases

Often robust stability in the face of change in a single parameter is of critical importance. In such cases, the uncertainty structure and the associated perturbed model can be further refined to obtain a tight upper bound on the minimum destabilizing perturbation. The key is to recognize that an additive model of parametric uncertainty of a single parameter $p_\delta = p_0\,(1+\delta)$ induces a particular structure of the perturbed model that combines multiplicative and inverse multiplicative uncertainty [19]

$$G_p^{i,j} = G_0^{i,j}\,\frac{1+W_{\mathrm{m}}^{i,j}\delta}{1+W_{\mathrm{im}}^{i,j}\delta}.$$

If δ is known for different tests, the unknown weights can be calculated on a frequency-by-frequency basis from measurements to fit this particular disturbance model. For instance, with three measurements available, one of them can be taken as a nominal plant, and the weights can be recovered for each input-output pair from the remaining measurements as follows

$$\begin{bmatrix} W_{\mathrm{m}}^{i,j}\,(j\omega_k) \\ W_{\mathrm{im}}^{i,j}\,(j\omega_k) \end{bmatrix} = \begin{bmatrix} -G_0^{i,j}\,(j\omega_k)\,\delta_1 & G_{p1}^{i,j}\,(j\omega_k)\,\delta_1 \\ -G_0^{i,j}\,(j\omega_k)\,\delta_2 & G_{p2}^{i,j}\,(j\omega_k)\,\delta_2 \end{bmatrix}^{-1} \begin{bmatrix} G_0^{i,j}\,(j\omega_k) - G_{p1}^{i,j}\,(j\omega_k) \\ G_0^{i,j}\,(j\omega_k) - G_{p2}^{i,j}\,(j\omega_k) \end{bmatrix}.$$

The advantage is that Δ_{Z} now has the form of a repeated real perturbation δI. Evaluating μ_Δ in this case is straightforward, since

$$\det(I - M\Delta_{\mathrm{Z}}) = (1-\delta\lambda_1(M))\cdots(1-\delta\lambda_n(M)). \quad (7)$$

Thus, minimum destabilizing perturbation can be estimated from the eigenvalue loci plots.

VI. Numerical Example and Results

The numerical example of this section aims to demonstrate the application of the robust stability analysis methodology for the case of SSCI between Type-III wind turbines and a series-compensated network. The benchmark system used for the study consists of an aggregated wind park with 66 wind turbines with nominal power of 1.7 MW each. The wind park is connected to a grid through a series-compensated transmission line. The details of the study case are found in [4], [20].

The grid impedance at PCC is measured for 4 levels of series compensation: 4%, 6%, 8% and 10%. The WPP admittance for the nominal power is measured as well. The frequency response is obtained for both dq domain and the the $\alpha\beta$ domain using the CTF modelling approach of (6). Following these measurements, the general procedure of Section V-A is applied. The stability of the nominal interconnection is assessed first using the eigenvalue loci plots for both impedance representations. Results of Fig. 4 show that the eigenvalue loci do not encircle the "-1" point. This confirms nominal stability for both models, according to the generalized Nyquist stability criterion. Note that both grid and wind park models are asymptotically stable.

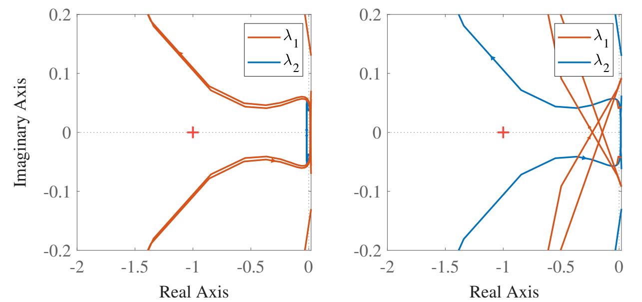

(a) $\alpha\beta$ domain (b) dq domain

Fig. 4: Eigenvalue loci plots for nominal plants modeled in different domains.

Next, the perturbed model plant is constructed, and associated calculation of the SSV is performed for different combinations of operating conditions, which in this case differ by the series compensation level. The SSV upper bound is calculated using the `mussv` function in `Matlab`. The results are shown in Fig. 5.

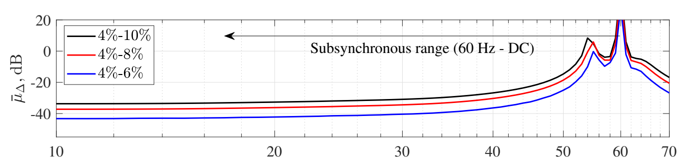

(a) dq domain model

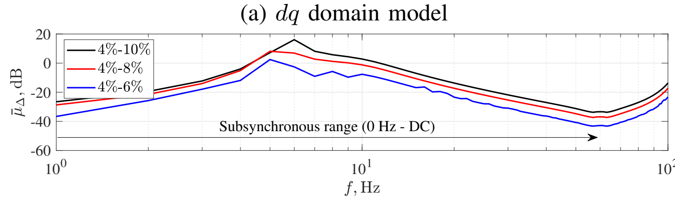

(b) $\alpha\beta$ domain model

Fig. 5: SSV upper bounds for uncertain system.

Ignoring the evaluation of the SSV upper bound at DC (which corresponds to 60 Hz for the dq domain model and 0 Hz for the $\alpha\beta$ domain model) and focusing on the subsynchronous range, it can be seen that both results are in accordance with each other. The calculated SSV upper bound peaks at around 6 Hz (54 Hz for the dq domain model). In the case of $\alpha\beta$ domain model the upper bound is very close to but slightly above 1, suggesting that robust stability is not guarantied for the constructed perturbed model. Conversely, the analysis applied to the perturbed model in dq domain suggests robust stability for the compensation level up to 6%. Thus, despite having more structure in the $\alpha\beta$ domain,

979-8-3315-8138-1

the resulting SSV calculation reveals that in this case the dq domain provides slightly less conservative assessment.

Since in this study the exact perturbations are known as they correspond to varying the compensation levels, a more refined analysis of Section V-B can be applied. For instance, if 4% compensation is assumed as a nominal plant, then 6% and 8% correspond to δ of 0.5 and 1 respectively. These three measurements are enough to calculate the weights for each input-output pair transfer function. Then, according to (7) the critical eigenvalue can be calculated to estimate the minimum destabilizing perturbation. The results of this calculation for SSCI case study for the model in dq domain are shown in Fig. 6.

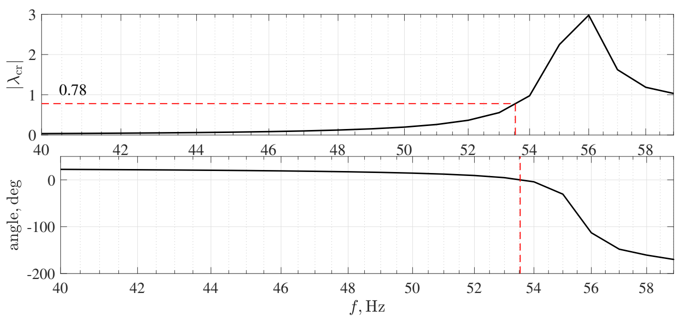

Fig. 6: Critical eigenvalue plot for SSCI case, dq domain

As can be seen, at zero crossing of the phase at the frequency of 53.5 Hz the eigenvalue magnitude is at 0.78, suggesting the minimum destabilizing perturbation of $\frac{1}{0.78} = 1.28$. This corresponds to the critical compensation level of $4 \cdot (1 + 1.28) = 9.13\%$. This agrees well with the results of [4] where for this study it was found that the critical compensation level is between 9% and 10%. Note that operating point corresponding to unstable conditions was not even used in the analysis, yet the prediction of the critical compensation level is very precise.

VII. Conclusions

A lack of systematic robust stability assessment techniques is a downside of impedance-based stability assessment methods. This paper demonstrates that the SSV analysis is a useful tool that can provide meaningful robustness metrics. When no information about the perturbation source is given, a general procedure is formulated, typically producing conservative results. In this case the only means of reducing the conservatism might be the choice of the domain in which the impedance is modelled. However, the results of the study case confirm that there is no obvious choice between dq and $\alpha\beta$ domains, even for symmetric grid models.

When the source of the uncertainty is a single parameter variation that is known, SSV analysis can be reduced to analyzing the eigenvalue loci, therefore providing accurate evaluation of the stability margins. This is useful in practice for interconnection studies for which a particular phenomenon is of concern, such as SSCI interactions between Type-III wind turbines and series-compensated grids.

Acknowledgment

The authors would like to thank AS Trevisan for making his code and models available for use.

References

[1] O. Saad, H. Honvo, A. Ajaja, S. Dennetière, and Y. Vernay, "Battery energy storage system integration to the RTE network: from EMT studies to site validation," in *22nd Wind and Solar Integration Workshop (WIW 2023)*, vol. 2023. IET, 2023, pp. 198–204.

[2] P. Le-Huy and O. Tremblay, "Hybrid SVC-VSC modeling approaches for hardware-in-the-loop simulation," *Electric Power Systems Research*, vol. 223, p. 109651, 2023.

[3] D. Rimorov, O. Tremblay, J.-F. Haché, V. Morissette, C. Desbiens, J. Lacroix, and P.-L. Martel, "Power-Hardware-in-The-Loop testing of residential PV inverters in the conditions of weak network," in *2020 IEEE Power & Energy Society General Meeting (PESGM)*. IEEE, 2020, pp. 1–5.

[4] A. S. Trevisan, A. Mendonca, R. Gagnon, J. Mahseredjian, and M. Fecteau, "Analytically validated SSCI assessment technique for wind parks in series compensated grids," *IEEE Transactions on Power Systems*, vol. 36, no. 1, pp. 39–48, 2020.

[5] S. Shah and L. Parsa, "Impedance modeling of three-phase voltage source converters in DQ, sequence, and phasor domains," *IEEE Transactions on Energy Conversion*, vol. 32, no. 3, pp. 1139–1150, 2017.

[6] J. Sun, "Impedance-based stability criterion for grid-connected inverters," *IEEE transactions on power electronics*, vol. 26, no. 11, pp. 3075–3078, 2011.

[7] A. Rygg, M. Molinas, C. Zhang, and X. Cai, "A modified sequence-domain impedance definition and its equivalence to the dq-domain impedance definition for the stability analysis of AC power electronic systems," *IEEE Journal of Emerging and Selected Topics in Power Electronics*, vol. 4, no. 4, pp. 1383–1396, 2016.

[8] L. Meng, U. Karaagac, and K. Jacobs, "A new sequence domain EMT-level multi-input multi-output frequency scanning method for inverter based resources," *Electric Power Systems Research*, vol. 220, p. 109312, 2023.

[9] A. A. Stoorvogel, S. Lotfifard, and A. Saberi, "On MIMO stability analysis methods applied to inverter-based resources connected to power systems," *arXiv e-prints*, pp. arXiv–2510, 2025.

[10] H. J. Marquez, *Nonlinear control systems: analysis and design*. Wiley-Interscience Hoboken, 2003, vol. 1.

[11] A. Packard and J. Doyle, "The complex structured singular value," *Automatica*, vol. 29, no. 1, pp. 71–109, 1993.

[12] L. Harnefors, X. Wang, A. G. Yepes, and F. Blaabjerg, "Passivity-based stability assessment of grid-connected VSCs—An overview," *IEEE Journal of emerging and selected topics in Power Electronics*, vol. 4, no. 1, pp. 116–125, 2015.

[13] W. M. Griggs, B. D. Anderson, and A. Lanzon, "A "mixed" small gain and passivity theorem in the frequency domain," *Systems & control letters*, vol. 56, no. 9-10, pp. 596–602, 2007.

[14] J. Forbes and C. Damaren, "Hybrid passivity and finite gain stability theorem: stability and control of systems possessing passivity violations," *IET control theory & applications*, vol. 4, no. 9, pp. 1795–1806, 2010.

[15] J. Doyle, A. Packard, and K. Zhou, "Review of LFTs, LMIs, and mu," in *[1991] Proceedings of the 30th IEEE Conference on Decision and Control*. IEEE, 1991, pp. 1227–1232.

[16] L. Harnefors, "Modeling of three-phase dynamic systems using complex transfer functions and transfer matrices," *IEEE Transactions on Industrial Electronics*, vol. 54, no. 4, pp. 2239–2248, 2007.

[17] X. Wang, L. Harnefors, and F. Blaabjerg, "Unified impedance model of grid-connected voltage-source converters," *IEEE Transactions on Power Electronics*, vol. 33, no. 2, pp. 1775–1787, 2017.

[18] S. Skogestad and I. Postlethwaite, *Multivariable feedback control: analysis and design*. john Wiley & sons, 2005.

[19] D. Rimorov, J. R. Forbes, O. Tremblay, and R. Gagnon, "Robust impedance emulation for transmission line interface in Power-Hardware-In-the-Loop applications: Optimal filter approach," *IEEE Open Journal of the Industrial Electronics Society*, 2025.

[20] A. Trevisan, M. Fecteau, A. Mendonça, R. Gagnon, and J. Mahseredjian, "Analysis of low frequency interactions between DFIG wind turbines and series compensated systems," in *Proc. IPST'19—Int. Conf. Power Syst. Transients*, 2019, pp. 1–7.

979-8-3315-8138-1